



BNL-104786-2014-TECH

AGS/AD/Tech Note No. 370;BNL-104786-2014-IR

A BROADBAND, HIGH ACCURACY PHASE SHIFTER

D. J. Ciardullo

January 1993

Collider Accelerator Department
Brookhaven National Laboratory

U.S. Department of Energy

USDOE Office of Science (SC)

Notice: This technical note has been authored by employees of Brookhaven Science Associates, LLC under Contract No.DE-AC02-76CH00016 with the U.S. Department of Energy. The publisher by accepting the technical note for publication acknowledges that the United States Government retains a non-exclusive, paid-up, irrevocable, world-wide license to publish or reproduce the published form of this technical note, or allow others to do so, for United States Government purposes.

DISCLAIMER

This report was prepared as an account of work sponsored by an agency of the United States Government. Neither the United States Government nor any agency thereof, nor any of their employees, nor any of their contractors, subcontractors, or their employees, makes any warranty, express or implied, or assumes any legal liability or responsibility for the accuracy, completeness, or any third party's use or the results of such use of any information, apparatus, product, or process disclosed, or represents that its use would not infringe privately owned rights. Reference herein to any specific commercial product, process, or service by trade name, trademark, manufacturer, or otherwise, does not necessarily constitute or imply its endorsement, recommendation, or favoring by the United States Government or any agency thereof or its contractors or subcontractors. The views and opinions of authors expressed herein do not necessarily state or reflect those of the United States Government or any agency thereof.

Accelerator Division
Alternating Gradient Synchrotron Department
BROOKHAVEN NATIONAL LABORATORY
Upton, New York 11973

Accelerator Division
Technical Note

AGS/AD/Tech. Note No. 370

A BROADBAND, HIGH ACCURACY PHASE SHIFTER

D. J. Ciardullo

January 4, 1993

INTRODUCTION:

Many systems operating at VHF frequencies and below require a method of varying the phase of an rf signal over a full 360 degrees. Often these applications require a device capable of broadband operation as well. While a myriad of phase shifters and modulators exist for this purpose at UHF and microwave frequencies, those available in the LF to VHF range tend to lack range, linear control and accuracy. This paper will focus on the concept of the vector modulator, which is capable of providing 360 degrees of unambiguous phase shift over a wide operating bandwidth. In addition, this type of device can provide a linear relationship between the control signal and resulting differential phase shift, while maintaining a constant output amplitude. Although the vector modulator concept is not new, advances in analog signal processing ICs have enabled the rf engineer to apply high speed linear techniques toward construction of phase shifters and modulators for use below UHF.

The purpose of this paper is to present a design for a high accuracy phase shifter based on the concept of the vector modulator. Basic theory will be introduced first, then applied to an actual design. Limitations of the main components of the design will be discussed, and test results for a typical "production" unit will be presented.

BASIC THEORY:

In a linear system, a constant amplitude sinusoidal signal can be represented as

$$f(t) = Ae^{st} = Ae^{j\omega t} \quad (1)$$

where s is the Laplace transform variable. Note that s is purely imaginary, and contains no real part with which to damp out the sinusoid (equivalent to a pair of poles lying on the $j\omega$ -axis in the complex plane). Since $f(t)$ is a complex function, the amplitude may also be complex;

$$A = Ae^{j\theta} \quad (2)$$

hence

$$f(t) = Ae^{j\theta} e^{j\omega t} = Ae^{j(\omega t + \theta)} \quad (3)$$

We will make use of two basic concepts¹ during the analysis of the vector modulator. The first is that the output of a linear circuit driven with a sinusoid will preserve the frequency of the input signal. The second concept states that the addition of two equal frequency sinusoids will result in another sinusoid of the same frequency. Combining these ideas, we see that a linear rf circuit (such as the vector modulator) will affect only the amplitude and phase of a sinusoidal input signal; The frequency at any point within the circuit will remain unchanged. In addition, the phase relationship between two signals of equal periodicity remains fixed, irrespective of when it is measured within the rf cycle. Thus for the purpose of analyzing the amplitude and phase of signals within the circuitry of the vector modulator, the $e^{j\omega t}$ term in Eq.[3] is somewhat redundant. This term can be eliminated by choosing an arbitrary time during the rf cycle with which to make comparisons (say, at $t=0$). Setting $t=0$ in Eq.[3] gives

$$f(t) = Ae^{j\theta} \quad (4)$$

which, when abbreviated as $A \angle \theta$ is known as *phasor notation*. A phasor diagram is simply a polar plot of directed lines (i.e., *phasors*) whose lengths are proportional to the amplitudes (A) of the signals being represented, with each phase (θ) measured relative to some reference. Since the vector modulator is a linear device, the analysis of its operation will be carried out using the method of phasors.

It is desired to create a system capable of manipulating the phase of a sinusoidal input signal. The ideal device would provide predictable, unambiguous phase shift of between 0° and 360° via electrical control signal. In addition, the output amplitude should remain constant, independent of the phase shift. Figure 1 is the block diagram of a device theoretically capable of achieving these goals.

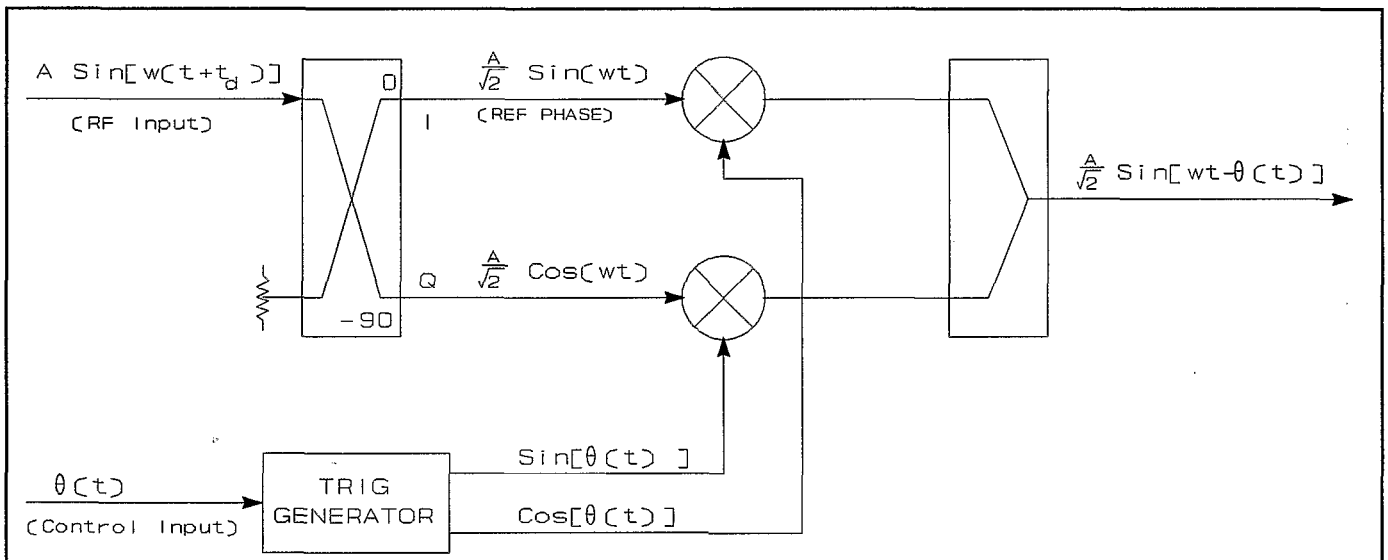


Figure 1. Basic Components of an Ideal Vector Modulator.

A 90° power splitter is used to decompose the input signal into two equal amplitude quadrature components, I (In-phase) and Q (Quadrature phase). The amplitude of each quadrature component is adjusted by multiplying it by some scaling factor between ± 1 . The scaled I and Q components are then combined vectorially, resulting in another sinusoid of equal frequency. This resultant will in general have amplitude and phase characteristics which differ from the original input signal. If the two scaling factors are represented by $\alpha(\Theta)$ and $\beta(\Theta)$, then the vector sum of the scaled I and Q components is

$$MAG: \sqrt{\left[\alpha(\Theta) \frac{A}{\sqrt{2}} \right]^2 + \left[\beta(\Theta) \frac{A}{\sqrt{2}} \right]^2} = A \sqrt{\frac{\alpha^2(\Theta) + \beta^2(\Theta)}{2}} \quad (5)$$

$$PHASE: \theta = \text{TAN}^{-1} \frac{\beta(\Theta)}{\alpha(\Theta)}$$

By independently adjusting the amplitude of each component, it is possible to obtain a resultant of any phase between 0°-360°. Since the two signals are "amplitude modulated" then vector summed, this phase shifting scheme is often referred to as "vector modulation".

To satisfy the previously defined requirements of predictable phase shift with constant output amplitude, it is necessary to scale each quadrature rf component in a specific manner. We have effectively fulfilled the first requirement simply by defining α and β as functions of the desired phase shift angle. The latter requirement, however, mandates the use of a quadrature pair of scaling functions whose vector sum is a constant magnitude (refer to Eq.[5]). A pair of functions satisfying these criteria may be found from the definition of the unit circle; $\text{Sin}^2(\Theta) + \text{Cos}^2(\Theta) = 1$. These two functions are orthogonal, and both depend on the phase shift angle, Θ . Substituting $\alpha(\Theta) = \text{Cos}(\Theta)$ and $\beta(\Theta) = \text{Sin}(\Theta)$ into Eq.[5] we obtain:

$$MAG: A \sqrt{\frac{\text{Cos}^2(\Theta) + \text{Sin}^2(\Theta)}{2}} = \frac{A}{\sqrt{2}} \quad (6)$$

indicating that the resultant amplitude is independent of the phase shift angle. Simultaneously scaling the amplitude of $\text{Sin}(\omega t)$ [the I component of the RF] by $\text{Cos}(\Theta)$, and $\text{Cos}(\omega t)$ [the Q component of the RF] by $\text{Sin}(\Theta)$ will therefore result in a constant amplitude sinusoid of predictable phase. Figure 2 illustrates how these scaling factors are used to manipulate the phase of the RF by solving the following trigonometric identity:

$$\text{Cos}(\Theta) \text{Sin}(\omega t) - \text{Sin}(\Theta) \text{Cos}(\omega t) = \text{Sin}(\omega t - \Theta) \quad (7)$$

The *Control Phasor*, which represents the desired phase shift Θ , is decomposed into its quadrature components [$\text{Sin}(\Theta)$, $\text{Cos}(\Theta)$]. These control components can now be used to scale the I [$\text{Sin}(\omega t)$] and Q [$-\text{Cos}(\omega t)$] RF signals, which are also 90° apart in phase. The top half of Figure 2 shows the components of both the phase control signal and the RF input. The quadrature components of both signals are multiplied together, and the resulting components vector summed to obtain a phase-shifted version of the

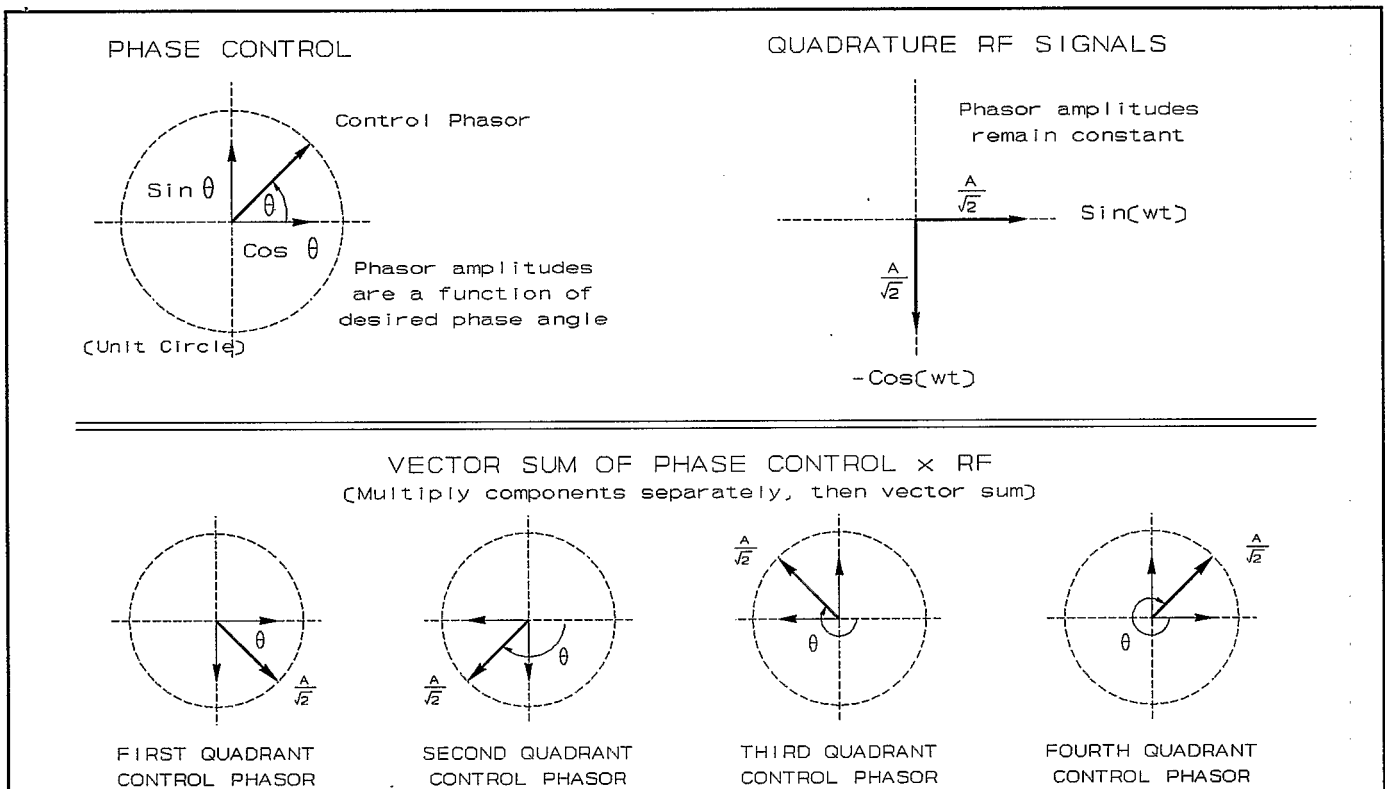


Figure 2. Phasor Representations showing $\text{Cos}(\theta) \text{Sin}(wt) - \text{Sin}(\theta) \text{Cos}(wt) = \text{Sin}(wt-\theta)$.

original RF input signal. Since both the Sine and the Cosine of the phase shift angle may take on negative values, the output of the vector modulator may have a resultant in any of the four quadrants (0° to -360°). The bottom half of Figure 2 is a sequence of four phasor diagrams illustrating the resultant output for four different phase shift settings. The sequence is from left to right with each diagram representative of the control phasor in a different quadrant. Note that for positive phase shifts the control phasor moves counterclockwise, while the output phasor moves clockwise.

PRACTICAL LIMITATIONS:

Each individual component shown in Figure 1 makes some contribution to the total amplitude and phase error of the output signal. The trigonometric identity in Eq.[7] may be used to analyze the extent of these contributions. In words, Eq.[7] states that two quadrature RF signals are scaled as the Sine and Cosine of the desired phase shift angle, then vector summed. Since we are using phasor analysis, it is natural to separate the total vector modulator output error into two basic categories, scaling (amplitude) inaccuracies and quadrature phase error. We will define *Scaling error* as the cumulative effect of multiplier inaccuracy, lack of trigonometric conformance (of the Sine and Cosine control signals), and any amplitude imbalance from the 90° divider or in-phase combiner. *Quadrature error* is primarily due to the 90° power divider, but can also include any phase imbalance of the 0° combiner used to execute the vector sum. Both categories contribute to the total phase and amplitude inaccuracy of the output signal.

Effect of Scaling Error:

In principle, the scaling factors of both quadrature RF phasors shown in Figure 2 will vector sum to a constant amplitude. Each of the major components shown in Figure 1, however, can potentially affect

the amplitude of one or both RF signals. The scale factors for each of the phasors is shown in Figure 2:

$$\begin{aligned} \text{Sin}(wt) \text{ Scale Factor: } & \frac{A}{\sqrt{2}} \text{Cos}[\theta(t)] \\ \text{Cos}(wt) \text{ Scale Factor: } & \frac{A}{\sqrt{2}} \text{Sin}[\theta(t)] \end{aligned} \quad (8)$$

At this point, the assumption is made that we are predominantly interested in the constancy of the output level, and not its absolute amplitude. To this end, Figure 3(a) illustrates a general scaling error where the ratio of the two phasor amplitudes is given as K. The two phasors are in this case of unequal amplitude, but are assumed to be in perfect quadrature. The effects of cumulative scaling error on the output signal can again be found using vector addition:

$$\begin{aligned} \text{MAG: } A_o[\theta, t, K] &= \sqrt{\left[\frac{A}{\sqrt{2}} \text{Cos}[\theta(t)] \right]^2 + \left[K \frac{A}{\sqrt{2}} \text{Sin}[\theta(t)] \right]^2} \\ &= \frac{A}{\sqrt{2}} \sqrt{\text{Cos}^2[\theta(t)] + K^2 \text{Sin}^2[\theta(t)]} \end{aligned} \quad (9)$$

$$\text{PHASE: } \phi[\theta, t, K] = \text{Tan}^{-1} [K \text{Tan}[\theta(t)]]$$

where: A_o is the actual output amplitude
 ϕ is the actual output phase shift
 Θ is the desired phase shift

resulting in an output signal $A_o \text{Sin}(wt + \phi)$, where both A_o and ϕ are assumed to be functions of the desired phase shift, time, and the RF amplitude imbalance. The time dependence is applicable only when the device is used as a phase *modulator*; For DC phase shifts there is no time dependence, and $\Theta(t)$ may be replaced with Θ in the above relations.

If K is chosen to be always greater than unity, then $K(A/\sqrt{2})$ will represent the larger amplitude axis (refer to Figure 3(a)). Equation [9] reveals that the maximum output amplitude error due to this effect occurs at values of Θ which cause the resultant to approach the larger amplitude axis. For example, in the case of Figure 3(a) the maximum error occurs when Θ is either 90° or 270° , since the vertical is the larger of the two axes. The effect of amplitude balance on the output phase error is not quite as obvious, however. If the output phase error ($\phi - \Theta$) is plotted against the requested phase shift (Θ), the maximum *absolute* phase error will occur near 45° for "small" values of K (i.e., less than 10%).

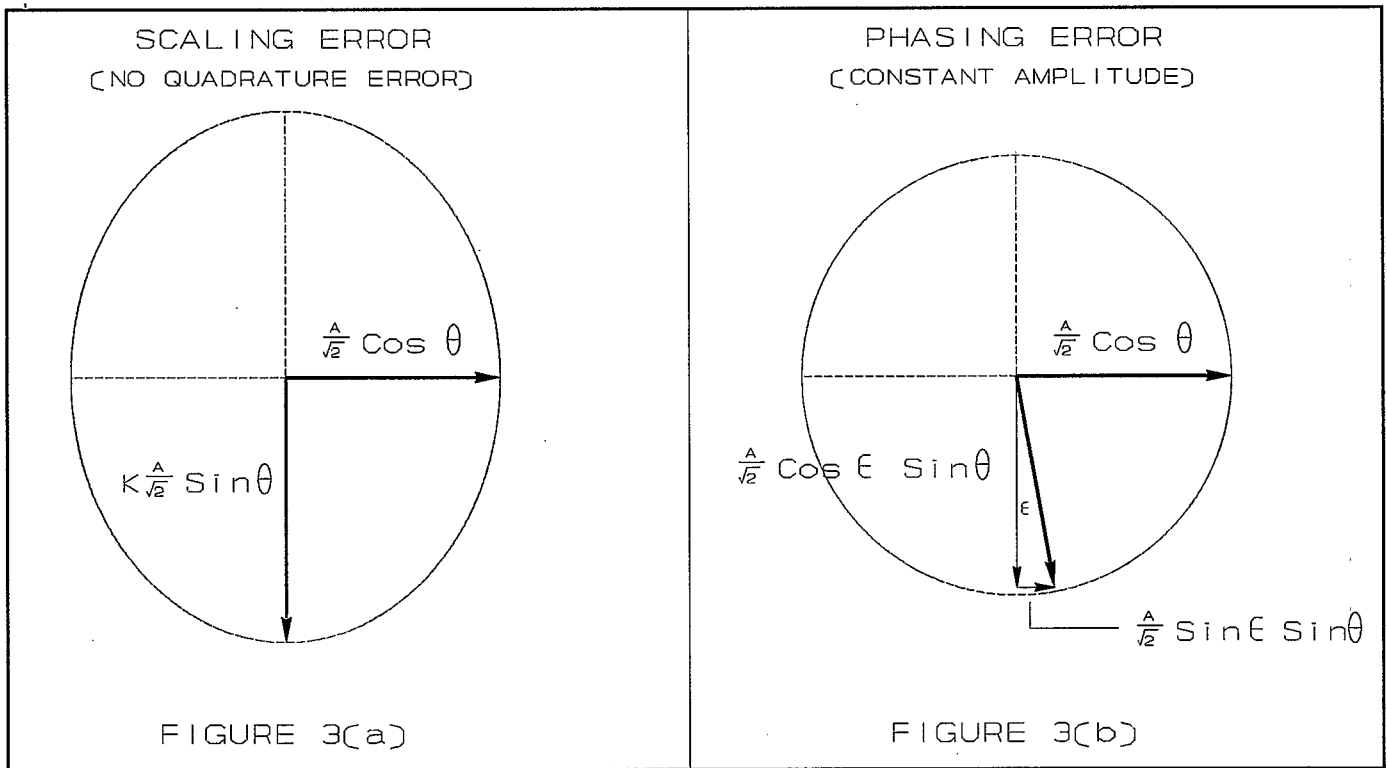


Figure 3. Phasor Diagrams Showing the Effects of (a) Scaling Error and (b) Phasing Error.

Effect of Quadrature Error:

For analysis purposes, phase imbalances from both the 90° divider and the in-phase combiner will be lumped into one effect. Figure 3(b) illustrates a non-quadrature phase division of the vector modulator input signal. The two phasors are assumed to be of equal amplitude and slightly out of quadrature, with ϵ degrees deviation from 90°. The effects of this type of error on the output signal can be found using vector addition:

$$\begin{aligned}
 \text{MAG: } A_o[\theta, t, \epsilon, \omega] &= \sqrt{\left[\frac{A}{\sqrt{2}} \cos[\theta(t)] + \frac{A}{\sqrt{2}} \sin[\epsilon(\omega)] \sin[\theta(t)] \right]^2 + \left[\frac{A}{\sqrt{2}} \cos[\epsilon(\omega)] \sin[\theta(t)] \right]^2} \\
 &= \frac{A}{\sqrt{2}} \sqrt{1 + \sin[2\theta(t)] \sin[\epsilon(\omega)]}
 \end{aligned} \tag{10}$$

$$\text{PHASE: } \phi[\theta, t, \epsilon, \omega] = \tan^{-1} \left[\frac{\sin[\theta(t)] \cos[\epsilon(\omega)]}{\cos[\theta(t)] + \sin[\theta(t)] \sin[\epsilon(\omega)]} \right]$$

where A_o , ϕ and Θ are defined as in Eq.[9]. Note that the output signal in this case is a function of the desired phase shift, time, quadrature phase error and frequency. The frequency dependence of ϵ is included to reflect the non-constant phase vs. frequency characteristics generally associated with broadband combiners and dividers (especially those providing quadrature phase splits). Inspection of Eq.[10] reveals that the maximum output phase error occurs when Θ is at 90°, while the amplitude error is greatest when Θ is at multiples of 45°.

THE ACTUAL VECTOR MODULATOR CONSTRUCTED:

Circuit Options

The relevant BNL drawing numbers for the vector modulator constructed are (note that these drawings are subject to further revisions/improvements):

PWB Assembly:	D36-E806 -4
Schematic:	D36-E804 -4

It was desired to build a general purpose, broadband phase shifter which could be utilized in a variety of rf and instrumentation applications. To achieve this goal, the device was designed with several input, output and control options which provide maximum flexibility while minimizing the amount of specialized hardware required for multiple applications.

The phase shifter can be configured to accept either a single rf input, or separate quadrature inputs. The first option is useful for applications requiring a relatively narrowband, "stand-alone" phase shifter. The PC board has been designed to accommodate standard 90° power dividers packaged in 8-pin relay cans, which are readily available from several popular rf component distributors. For wider bandwidth applications, the quadrature input option allows the use of an external 90° splitter to provide the quadrature phase relationship of the input signals. In this mode, the device can be used in conjunction with a variety of "off the shelf" wideband 90° hybrids. This option is also useful when the phase shifter is to be used in a system employing Direct Digital Synthesis (DDS) techniques. Quadrature DDS signals are noted for their superior linear phase characteristics, as well as their excellent amplitude and phase balance. To accommodate both rf input options, the main body of the vector modulator has been designed to operate from 100 KHz to 250 MHz.

Options have been provided for either analog or digital phase shift control. When used in the analog control mode, the device can be used as either a phase shifter or a linear phase modulator (with modulation frequencies to 1MHz). The control input may span ± 10 Volts, and has the effect of adding (negative control voltage) or subtracting (positive control voltage) 50° of phase shift per volt. When configured for digital control, an on-board DAC is used to provide accurate, stable voltage control for phase shifts of 0° (h000) to 511° (h1FF).

The phase shifter constructed also has two output options. The first is the more commonly utilized rf sinusoidal output (into 50 Ω). The alternative option provides a TTL output for interfacing the device with digital timing systems. When used in this mode, the main body of the phase shifter is capable of operation from DC (when used with DDS quadrature inputs) to > 10 MHz.

Choice of Components:

The circuit element used to decompose the input signal of the vector modulator into equal-amplitude quadrature components depends on several factors. Device characteristics such as amplitude imbalance, phase deviation from 90° and group delay flatness must all be considered before the proper phase splitting element can be selected. The extent to which the two signals are in quadrature affects both the phase accuracy and amplitude of the overall vector modulator (*Quadrature Error*). In addition, the amplitude balance of the two quadrature outputs contributes to the overall *Scaling Error*, causing additional phase and amplitude inaccuracy of the output signal.

For applications where flat group delay (deviation from linear phase) is not critical, the most popular circuit element used to phase split the input signal is the 90° power divider. Today there are many high quality passive broadband 90° hybrids available with good amplitude and phase balance. Alternatively, if the phase shifter is supplied with quadrature inputs from a Direct Digital Synthesizer, much higher phase accuracy, phase independent output amplitude, and linear phase can be achieved. For frequencies in the HF band and below, a compromise may be struck by using high speed active all-pass filters to achieve the 90° phase split with excellent amplitude balance and a relatively small amount of phase ripple. The phase shifter constructed has the flexibility of utilizing signals from any of the above mentioned sources.

As shown in Figure 1, two multiplying elements are needed to amplitude modulate the quadrature rf signals by the Sine and Cosine of the desired phase shift angle. These devices must be linear over the bandwidth of interest, with minimal dc offset errors. Any gain mismatch between the two multipliers will contribute to the overall *scaling error* of the vector modulator. The circuit elements used in the phase shifter are a pair of high speed 4-quadrant multipliers (Analog Devices AD834), chosen for their DC-500 MHz frequency response, high linearity, and ease of use. In addition to their extremely broad bandwidth, these multipliers have two important advantages over the use of current controlled attenuators.² The inputs to the device are voltage driven, eliminating the need for V-I conversion of the Sine and Cosine modulating signals. Vector summing the outputs of both multipliers is accomplished by simply paralleling their differential current outputs. This current combining technique helps to extend the bandwidth of the phase shifter, while greatly reducing any phase and amplitude imbalances which might be introduced by using an rf power combiner for the same purpose. The simplified transfer function for the multiplier is $I_o = V_{i1} V_{i2} (4\text{ma})$, giving a peak output current of 4ma for peak input voltages of $V_{i1} = V_{i2} = 1\text{V}$. A broadband center-tapped transformer (Mini-Circuits T4-6T, 20 KHz-250 MHz) is used to convert the differential vector sum to a single-ended 50 Ohm signal. A 12 dB amplifier (Avantek model GPD-130, TO-39 package, 100 KHz-400 MHz) is used to compensate for the decrease in voltage level effected by the transfer function of the multipliers. This combination of transformer and rf amplifier produces the upper and lower bandwidth constraints for the main body of this phase shifter. These parts can be easily modified, however, to reflect operating frequency requirements other than those used here.

When the phase shifter is configured for the TTL output option, the transformer and rf amplifier are not utilized. Instead, a high speed TTL comparator is used as the output driver. The comparator used (Analog Devices AD790) was chosen for its high common mode input voltage, necessary to accommodate the voltages resulting from the quiescent current of the multiplier outputs.

In order to achieve a constant output amplitude signal whose phase is linearly related to the control input, the *trigonometric generator* block (Figure 1) must provide the Sine and Cosine of the desired phase shift angle. Lack of trigonometric conformance causes both phase inaccuracy and amplitude variation in the output signal via scaling errors (Eq.[8]). There are several methods of obtaining the Sine and Cosine of the desired phase shift angle, including the use of Sine and Cosine potentiometers, digital look-up tables or trigonometric function generator ICs. For the phase shifter described by Figures 4 and 5, two high conformance trigonometric function generator ICs (Analog Devices AD639) are used. Given an input voltage $V(\Theta)$ scaled at 50°/Volt, one IC outputs a voltage which is proportional to $\text{Sin}(\Theta)$ and the other a voltage proportional to $\text{Cos}(\Theta)$. These ICs offer the flexibility of linear input voltage control, and can be driven via DAC, linear potentiometer or modulating waveform (dependent upon the control option selected). These devices also determine the highest angle modulation rate that can be achieved by the phase shifter.

The digital control option uses a 12-bit DAC with built-in voltage reference. By utilizing only the highest 9 bits, the DAC functions as an accurate, stable voltage input for the trigonometric generator ICs.

For "user friendliness" the gain of the DAC is adjusted such that 1 LSB corresponds to 1° of phase shift (DAC output of 20 mV/LSB).

RESULTS:

The phase shifter tested is configured for digital phase control, quadrature rf inputs (implying the use of an external hybrid or other source of quadrature signals) and 50 Ohm rf output. Test results are presented using the external hybrid option to illustrate the sensitivity of the vector modulator to the amplitude and phase balance of its quadrature inputs. To help illustrate this, results will be presented using two different quadrature hybrids; a commercially available 90° power divider and an active 90° all-pass network. Both hybrids exhibit similar non-linear phase characteristics and phase ripple, but the amplitude balance of the active circuit is an order of magnitude better than that of the passive device. In addition, the active circuit has a slightly smaller overall bandwidth.

The external 90° power divider used for these tests is a Merrimac model QH-7-4.9. Network analyzer plots of the amplitude and insertion phase for this hybrid are presented in Figure 4 (note that the phase response is not linear with frequency). Figure 5(a) shows the output of the phase shifter, using the QH-7-4.9 to supply the quadrature signal inputs. Time delay has been (mathematically) added to the network analyzer to help illustrate the degree of phase linearity (notice the similarity to the phase-frequency response of the hybrid). In Figure 5(b), the output of the phase shifter is normalized to the insertion phase of the hybrid. Once again, a pure delay has been added to the measurement for illustrative purposes. This relative measurement separates the group delay characteristic of the hybrid from that of the main body of the vector modulator. The sharp upward rise at the bottom end of the response occurs because of the low end roll-off of the GPD-130 used to boost the output signal.

Figure 6(a) shows the "worst case" output of the phase shifter for a requested shift of 45° . The relative amplitude balance of the hybrid is overlaid on the same plot to show its effect on the output phase error. Note that any phase imbalance from the hybrid also contributes to the total error at this requested shift, so there is not an exact one to one correspondence between the two plots in the figure. Figure 6(b) is a plot of the vector modulator output for a requested phase shift of 90° . The relative phase balance (deviation from quadrature) of the hybrid is overlaid on the same plot to show how closely the output phase error follows that of the 90° divider. These plots, together with equations 9 and 10, illustrate how the phase shifter output error is primarily a function of the amplitude and phase balance associated with the 90° hybrid (both plots have been normalized to the insertion phase of the QH-7-4.9).

The second group of plots result from using active all-pass networks to obtain the 90° phase split. The amplitude and phase balance for this circuit (one output normalized to the other) is presented in Figure 7. The amplitude balance is seen to be within 0.05dB (much less than that of the passive hybrid), and the deviation from quadrature phase is approximately $\pm 1^\circ$ from 300kHz to 7MHz. Figure 8(a) is a plot of the phase shifter output for a requested shift of 45° (top trace), normalized to the insertion phase of the active 90° all-pass network. For convenience, the phase balance is presented on the same plot (bottom trace). Notice that the shape of the output phase is a scaled version of the bottom trace; The relatively tight amplitude balance of the quadrature splitter contributes a negligible amount to the total output phase error. Figure 8(b) is a plot of the output for a requested shift of 90° (top trace) and the phase balance of the active splitter (bottom trace). Note the almost one to one correspondence between the shape factors of both traces.

Figure 9(a) shows the phase shifter output normalized to the insertion phase of the active splitter. The bottom trace in Figure 9(b) is an expanded view ($2^\circ/\text{div}$) for a requested shift of 0° . This plot shows the contribution that the main body makes to the total phase non-linearity of the vector modulator (a delay has been added mathematically to "flatten out" the linear phase portion of the response for illustrative purposes). Again, the rise at the low end of the response results from being close to the low frequency roll-off of the amplifier used (100 kHz). The plot in Figure 9(b) shows the insertion phase of the entire vector modulator, including the active splitter (top trace).

CONCLUSION:

A design for a high accuracy broadband phase shifter based on the concept of the vector modulator has been presented. The design is flexible enough to allow either digital or analog phase shift control, allowing the device to be used as a high linearity phase modulator. Using currently available analog processing components, the design achieves its goal of broadband, linear phase control for shifts well in excess of 360° (digital control input option). The device is also capable of being controlled via analog input voltage (or modulating waveform), resulting in phase excursions of up to $\pm 500^\circ$. The accuracy of the phase shifter (including both output amplitude and phase) has been shown to rely heavily on the amplitude and phase imbalances associated with the 90° phase splitting device used. In addition, the group delay of the quadrature phase splitter directly affects the delay characteristics of the phase shifter. For linear-phase sensitive applications, the use of either DDS techniques (successfully implemented, but not shown here) or linear phase all-pass structures may be employed to provide the required I and Q inputs to the vector modulator. For applications not requiring flat group delay, many "off the shelf" quadrature power dividers are available to serve the same purpose.

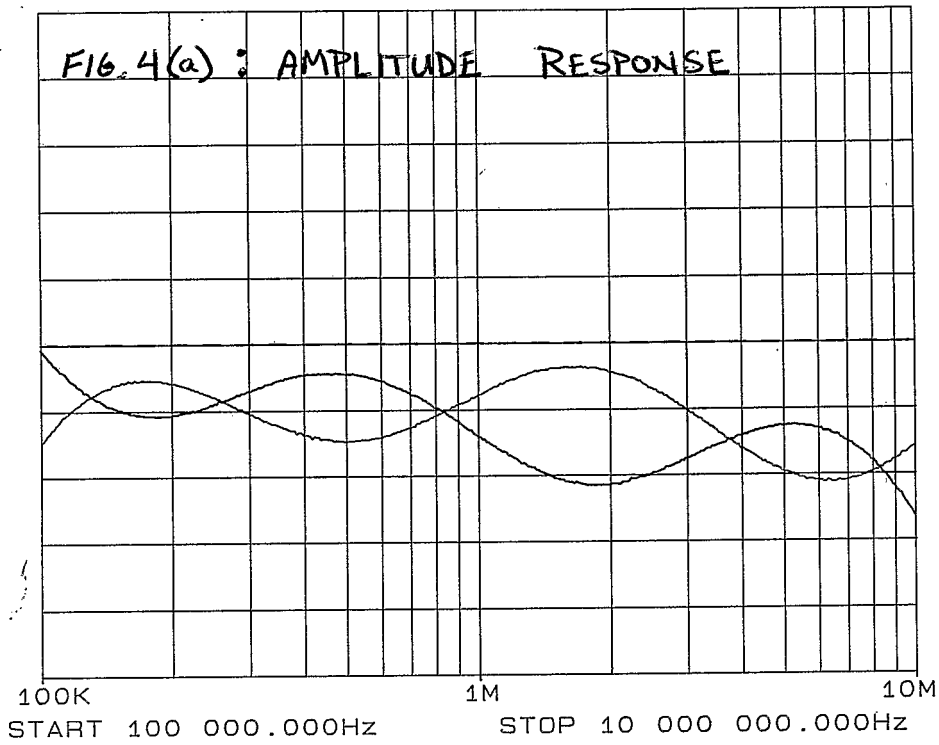
ACKNOWLEDGEMENT:

The assistance of T. Hayes in the review of this technical note is gratefully acknowledged.

REFERENCES:

1. Lynch, W.A.; Truxal, J.G.; Introductory System Analysis, McGraw-Hill Book Company, 1961, New York, pp. 22-31.
2. Perica, G.; "Voltage-Controlled RF Phase Shifter", in *Microwave Journal*, July 1986, pp. 166-168.
3. Hostetter, G.H.; Fundamentals of Network Analysis, New York, Harper & Row, Inc., 1980, pp. 337-344.

REF LEVEL /DIV
 -3.000dB 0.500dB
 -3.000dB 0.500dB



REF LEVEL /DIV
 150.000deg 45.000deg
 150.000deg 45.000deg

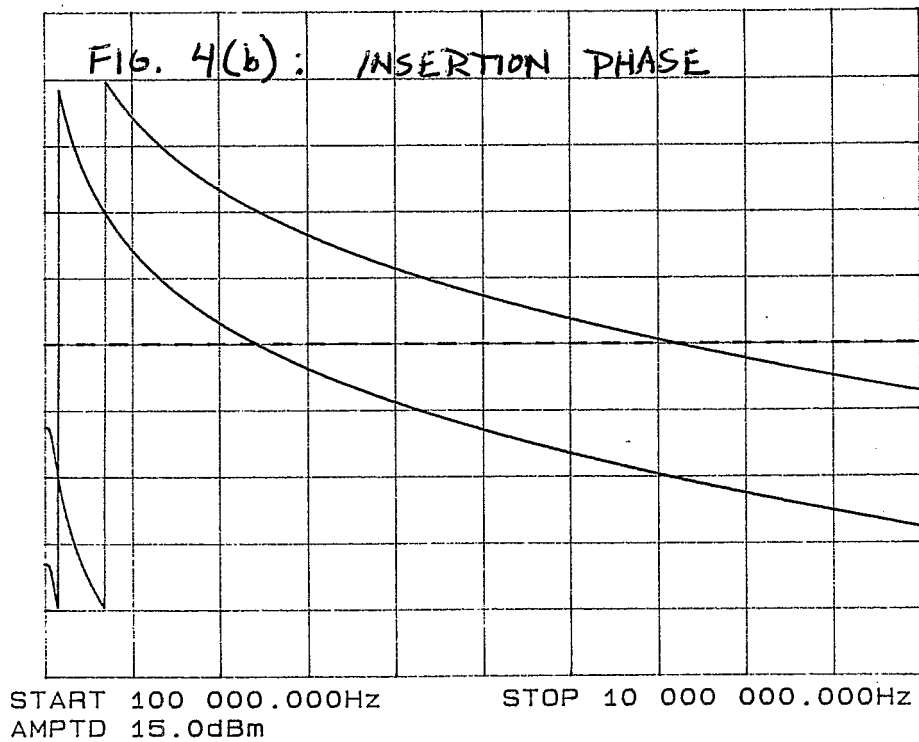
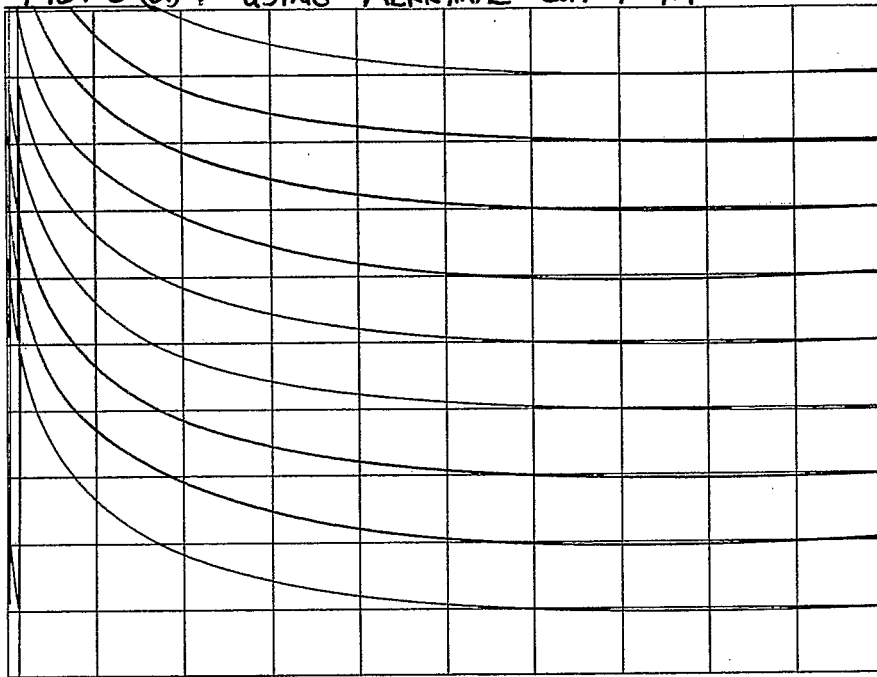


FIGURE 4 AMPLITUDE & PHASE RESPONSE OF QH-7-4.9 HYBRID

REF LEVEL /DIV
-119.250deg 45.000deg

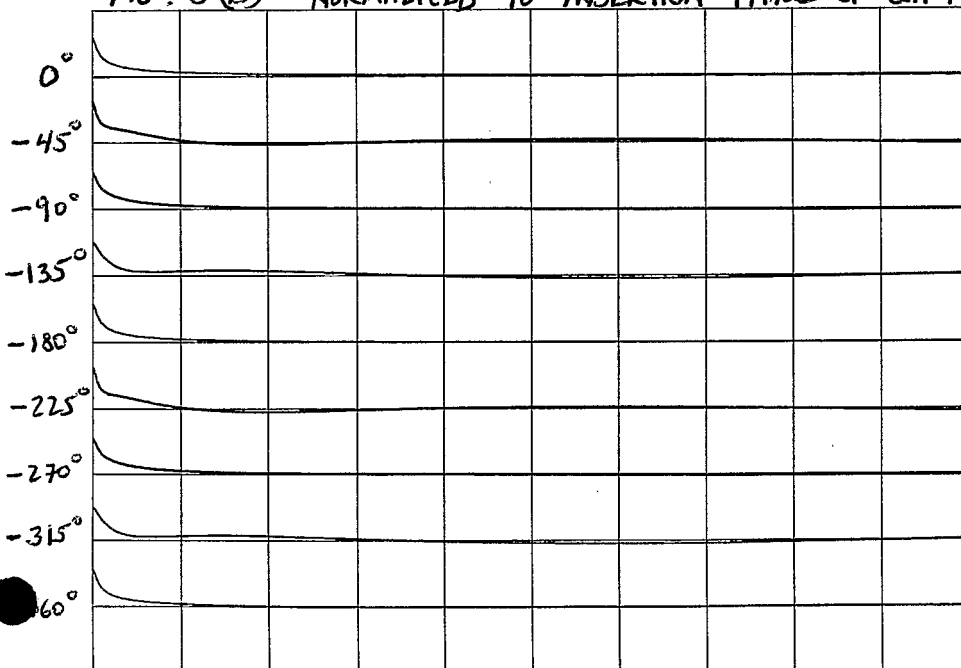
FIG. 5(a): OUTPUT OF PHASE SHIFTER
USING MERRIMAC QH-7-4.9



START 100 000.000Hz STOP 10 100 000.000Hz
AMPTD 15.0dBm

REF LEVEL /DIV
0.0deg 45.000deg

FIG. 5(b) OUTPUT OF PHASE SHIFTER,
NORMALIZED TO INSERTION PHASE OF QH-7-4.9.



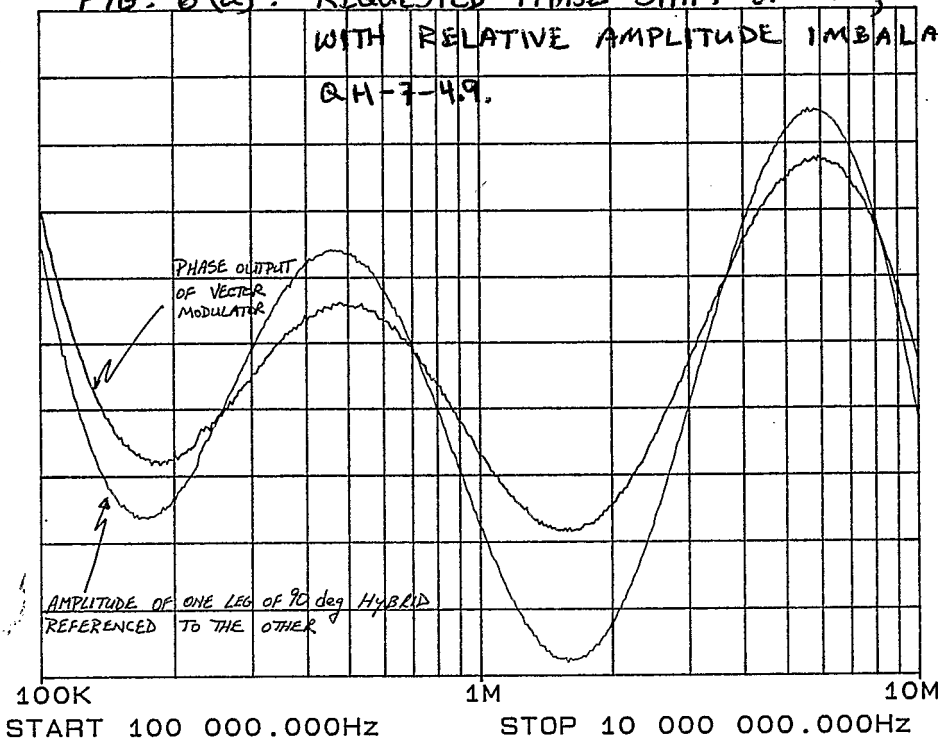
START 100 000.000Hz STOP 10 000 000.000Hz
AMPTD 15.0dBm

OUTPUT OF PHASE SHIFTER
USING QH-7-4.9 TO SUPPLY
QUAD. INPUTS

FIGURE 5.

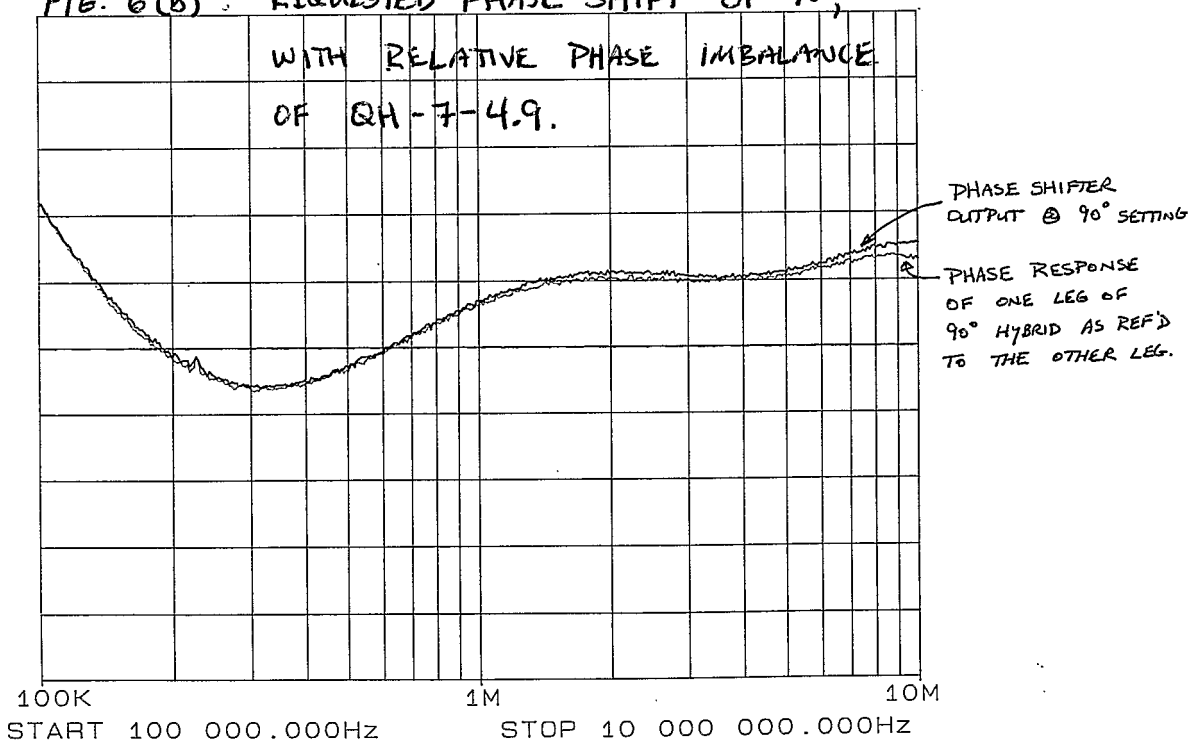
REF LEVEL /DIV
 45.000deg 1.000deg
 0.000dB 0.200dB

FIG. 6(a): REQUESTED PHASE SHIFT OF 45°,
 WITH RELATIVE AMPLITUDE IMBALANCE OF
 QH-7-4.9.



REF LEVEL /DIV
 90.000deg 1.000deg

FIG. 6(b): REQUESTED PHASE SHIFT OF 90°,
 WITH RELATIVE PHASE IMBALANCE
 OF QH-7-4.9.



(a) AMPLITUDE (SCALING) ERRORS
 (b) QUADRATURE ERRORS

"WORST CASE" PHASE SHIFTS FOR:

FIGURE 6.

REF LEVEL /DIV
0.000dB 0.100dB
-90.000deg 1.000deg

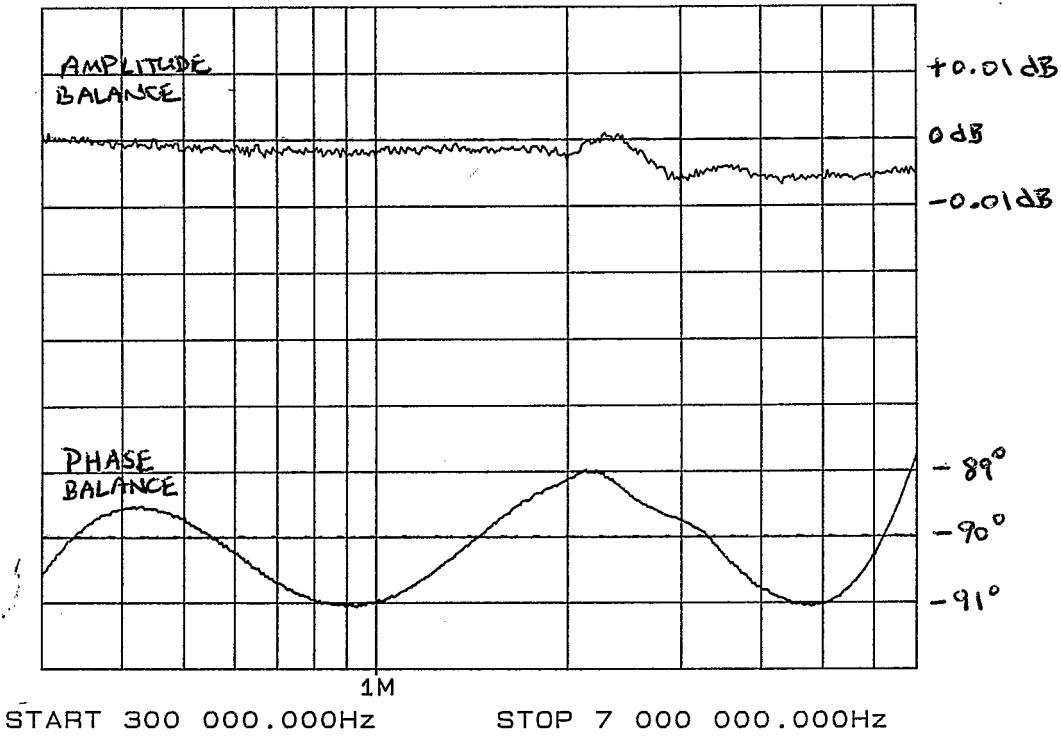
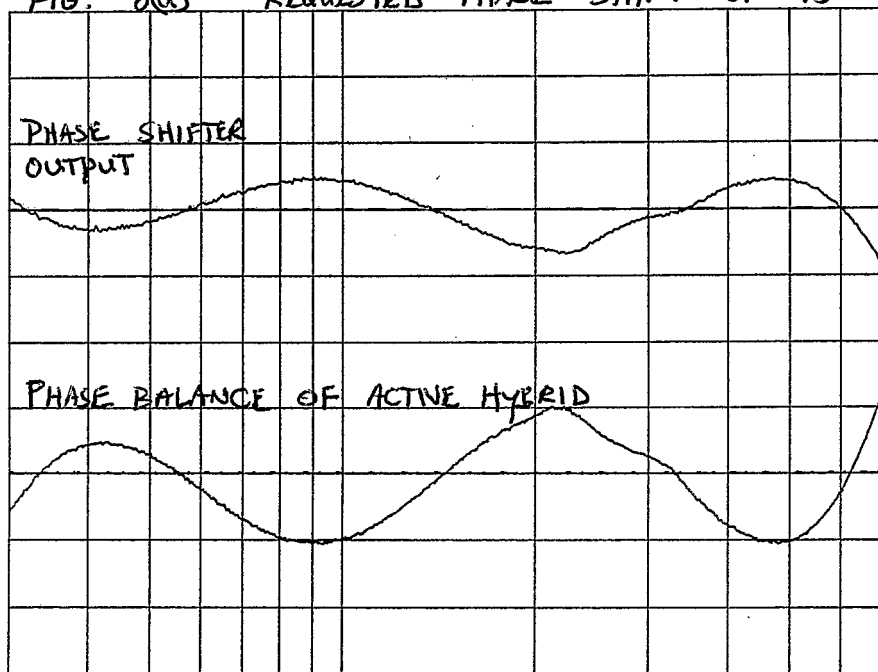


FIGURE 7. AMPLITUDE & PHASE BALANCE FOR ACTIVE HYBRID CIRCUIT

REF LEVEL /DIV
 45.000deg 1.000deg
 -90.000deg 1.000deg

FIG. 8(a) REQUESTED PHASE SHIFT OF 45°



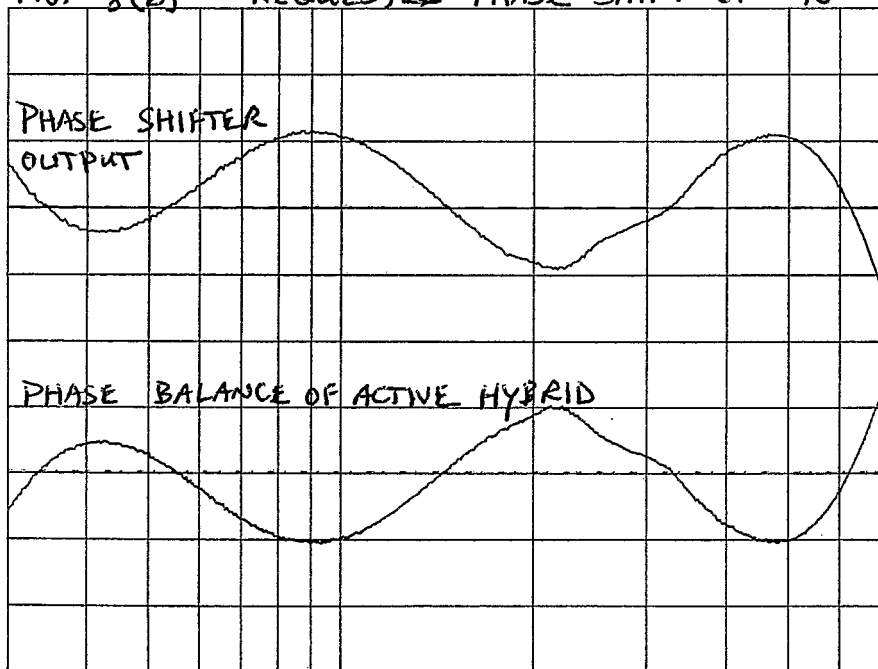
1M

START 300 000.000HZ

STOP 7 000 000.000HZ

REF LEVEL /DIV
 90.000deg 1.000deg
 -90.000deg 1.000deg

FIG. 8(b) REQUESTED PHASE SHIFT OF 90°



1M

START 300 000.000HZ

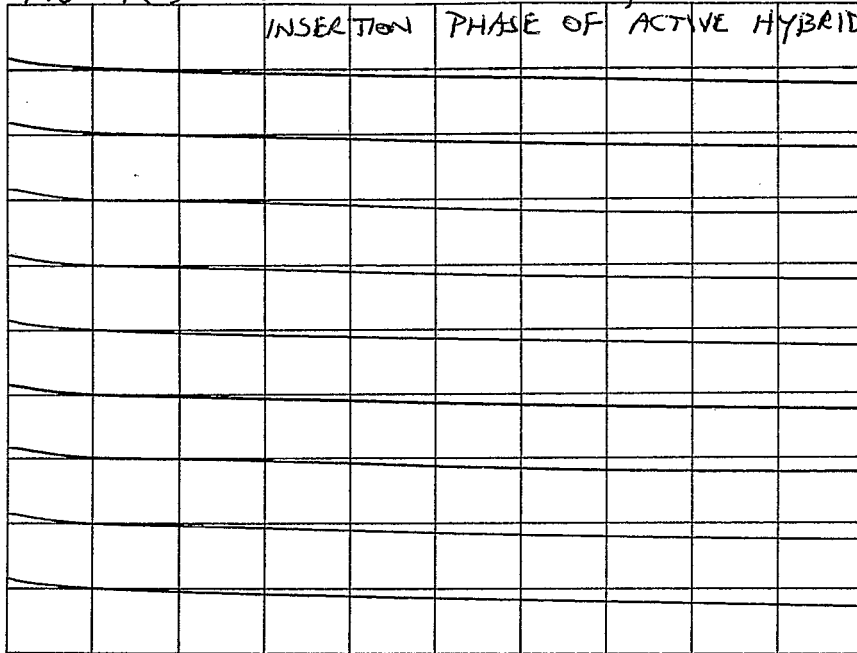
STOP 7 000 000.000HZ

FIGURE 8. "WORST CASE" PHASE SHIFTS FOR
 (ACTIVE HYBRID USED FOR 90° SPLIT)

(a) SCALING RELATED PHASE ERRORS
 (b) QUADRATURE ERRORS

REF LEVEL /DIV
 0.0deg 45.000deg

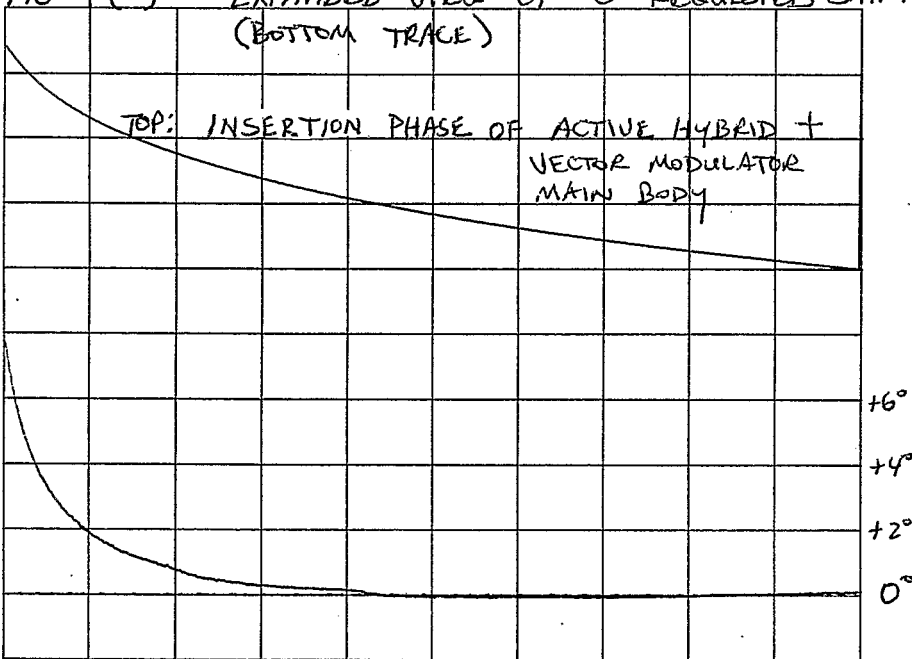
FIG. 9(a) PHASE SHIFTER OUTPUT, NORMALIZED TO



START 300 000.000HZ STOP 7 000 000.000HZ
 AMPTD 15.0dBm

REF LEVEL /DIV
 0.0deg 90.000deg
 0.0deg 2.000deg

FIG 9(b) EXPANDED VIEW OF 0° REQUESTED SHIFT
 (BOTTOM TRACE)



START 300 000.000HZ STOP 7 000 000.000HZ
 AMPTD 15.0dBm

PHASE SHIFTER OUTPUT, NORMALIZED TO
 INSERTION PHASE OF ACTIVE HYBRID.
 FIGURE 9.